Multiple well systems with non-Darcy flow

by Ana Mijic[1], Simon A. Mathias[2], and Tara C. LaForce[3]

[1]Corresponding author: Department of Earth Science and Engineering, Imperial College London, London, UK; ana.mijic08@imperial.ac.uk

[2]Department of Earth Sciences, Durham University, Durham, UK; s.a.mathias@durham.ac.uk

[3]CSIRO Earth Science and Resource Engineering, Clayton South, Victoria, Australia; tara.laforce@csiro.au

Abstract

Optimisation of groundwater and other subsurface resources requires analysis of multiple well systems. The usual modelling approach is to apply a linear flow equation (e.g. Darcy's law in confined aquifers). In such conditions the composite response of a system of wells can be determined by summating responses of the individual wells (the principle of superposition). However, if flow velocity increases, the nonlinear losses become important in the near-well region and the principle of superposition is no longer valid. This article presents an alternative method for applying analytical solutions of non-Darcy flow for a single well to multiple well systems. The method focuses on the response of the central injection well located in an array of equally spaced wells, as it is the well that exhibits the highest pressure change within the system. This critical well can be represented as a single well situated in the centre of a closed square domain, the width of which is equal to the well spacing. It is hypothesised that a single well situated in a circular region of the equivalent plan area adequately

represents such a system. A test case is presented and compared to a finite difference solution for the original problem, assuming the flow is governed by the nonlinear Forchheimer equation.

Introduction

The simulation of groundwater hydraulics requires a reliable tool for the prediction of fluid pressure distribution resulting from production and/or injection of fluids into subsurface formations (Schwartz and Zhang 2002). Easy to implement and computationally efficient, analytical solutions are often being considered a more practical approach to flow analysis. However, they are correct under simplifying assumptions made for their derivation.

Most relevant solutions have been designed for single-well systems situated in infinite aquifers. However, if the pressure buildup needs to be maintained below some limiting value (Rutqvist et al. 2008; Mathias et al. 2009a) it may be necessary to consider multiple well systems (MWS). For linear problems (Stephenson and Radmore 1990), solutions to MWS can be obtained by implementing the principle of superposition (Schwartz and Zhang 2002). In this article, flow linearity assumes the first order relationship between the fluid flux and pressure gradient, known as Darcy's law. Indeed, single phase and Darcy flow problems are often well described by linear sets of equations (e.g. Theis 1935; Mathias and Butler 2006). However, when one is interested in multiphase and/or non-Darcy flow, linearity no longer applies (Mathias et al. 2008, 2009b, Mijic and LaForce 2012). For such situations, an alternative method for MWS is required.

This article addresses the problem of water injection under non-Darcy flow in MWS. However, the same approach is appropriate for either injection or production well systems. With increasing flow velocity, inertial forces become significant and the linear relationship between pressure rise and the flow rate becomes invalid (Moutsopoulos et al. 2009). This flow condition is often described using the so-called Forchheimer (1901) equation.

Theoretical aspects of the Forchheimer equation are presented in studies of Irmay (1958), Ruth and Ma (1992), Whitaker (1996), Giorgi (1997) and Chen et al. (2001). Hassanizadeh and Grey (1987) derived the generalised form of the Forchheimer equation based on the fundamental laws of continuum mechanics, concluding that the nonlinear effects are due to significant viscous forces at high flow velocities. Non-Darcy flow has been confirmed in both coarse granular media (Thiruvengadam and Kumar 1997; Venkataraman and Rama Mohan Rao 1998, 2000; Legrand 1999; Chen et al. 2003; Reddy and Rama Mohan Rao 2006; Sidiropoulou et al. 2007) and fractured formations (Kohl et al. 1997; Lee and Lee 1999; Qian et al. 2005, 2007). Chen at al. (2003) analysed non-Darcy flow in horizontal wells and verified numerical results with data monitored on a physical laboratory model. More recently, Mathias and Todman (2010) demonstrated a formal link between the Forchheimer parameter and the so-called well-loss coefficient, associated with the analysis of step drawdown tests.

The non-Darcy regime can be identified either with the critical value of Reynolds number or Forchheimer number (Zimmerman et al. 2004; Zeng and Grigg 2006). Li and Engler (2001) present a comprehensive review of the correlations for the non-Darcy coefficient. They suggest a procedure for choosing the right correlation based on the formation lithology and the estimation of aquifer properties. Effects of nonlinear losses are the most significant in the near-well area, where high-velocity non-Darcy conditions occur (Mathias et al. 2008; Mathias and Todman 2010; Mijic and LaForce 2012).

Non-Darcy flow in single-well systems has been extensively studied in the past. Analytical solutions to steady state radial Forchheimer flow were obtained by Bear (1979) and Ewing et al. (1999). Although an exact solution to transient Forchheimer flow does not currently exist, some authors have developed approximate solutions (Sen 1988; Kelkar 2000; Wu 2002a; Mathias et al. 2008). A comprehensive set of analytical and semi-analytical solutions for the problem of transient Forchheimer flow to a single-well within an aquifer of infinite extent is presented in Mathias et al. (2008). Numerous studies address numerical simulations of non-Darcy flow using the Forchheimer equation. Some of them implement finite element approximation (Ewing et al. 1999; Kolditz 2001), while others apply finite difference approach (Holditch and Morse 1976; Choi et al. 1997; Wu 2002b; Belhaj et al. 2003; Mathias et al. 2008).

Note that most of solutions for non-Darcy flow specifically relate to confined aquifers. To account for the nonlinear flow behavior during a constant-head well test in an unconfined aquifer, Chen and Chang (2003) developed a curve matching method with the skin effect. Moutsopoulos (2007) implemented the Forchheimer equation to solve one-dimensional unsteady flow in an unconfined semi-infinite aquifer. More recently, Eck et al. (2012) developed an analytical solution for the Forchheimer seepage through an inclined porous layer under constant areal recharge.

Compared to the vast of literature on the modelling single-well systems, there is limited work on the modeling MWS. Nordbotten et al. (2004) analysed potential leakage of injected waste fluids through abandoned wells. Results of the study showed that leakage in a system of multiple passive wells in the vicinity of an injection well is nonlinear due to interaction between leaky wells. Consequently, the overall leakage rate per well in the system was reduced. Pech and Novotny (2005) and Novotny and Pech (2005) derived relations for a composite drawdown in case of MWS and wells near hydrological boundaries, respectively. In both studies, the principle of superposition was implemented in an analytical solution derived to include well skin losses. However, the accuracy of these results was not demonstrated by comparison with numerical simulation or experimental data. Mijic (2009) presented the analysis of MWS under steady state non-Darcy flow conditions. The obtained analytical solution can be used where there is no influence of the flow boundary on the pressure buildup at the well.

The work presented in this article seeks to further develop existing analytical solutions to account for the influence of the no-flow boundary in confined domains under non-Darcy flow conditions. Starting from the mass balance equation for slightly compressible flow, the analytical solution for Forchheimer flow and finite aquifer formations is derived. Furthermore, a hypothesis for the implementation of the obtained solution in the analysis of MWS is proposed. Performance of the solution is compared with the results from a numerical model of the original problem. The numerical model is developed using a finite difference approach, with variable grid spacing to accommodate convergence of flow lines near the production well. Finally, the applicability of the approach to unconfined aquifers is discussed.

Transient non-Darcy flow to a well in a closed aquifer

Non-Darcy flow conditions can be described using the Forchheimer (1901) equation

$$\frac{\mu q}{k} + \rho b|q|q = -\frac{dP}{dr} \tag{1}$$

where μ [ML^{-1}T^{-1}] is dynamic fluid viscosity, q [LT^{-1}] is fluid flux, k [L^{2}] is intrinsic permeability, ρ [ML^{-3}] is fluid density, P [ML^{-1}T^{-2}] is fluid pressure, r [L] is radial distance from the well and b [L^{-1}] is known as the Forchheimer parameter. For low fluid fluxes, Equation (1) reduces to Darcy's law.

The governing mass conservation equation for radial, slightly compressible flow in a homogenous, isotropic and confined aquifer with the injection well centrally located can be written as (Dake, 1983)

$$S_p \frac{\partial P}{\partial t} + \frac{1}{r}\frac{\partial}{\partial r}(rq) = 0 \tag{2}$$

where $S_p = \emptyset\left(c_r + c_f\right)$ [M^{-1}LT^{2}] is the pressure domain specific storage coefficient, t [T] is time since the beginning of injection, $\emptyset$ [-] is formation porosity and $c_r = \emptyset^{-1}(d\emptyset/dP)$ [M^{-1}LT^{2}] and $c_f = \rho^{-1}(d\rho/dP)$ [M^{-1}LT^{2}] are compressibility of the rock and fluid, respectively. The relevant initial and boundary conditions are

$$\begin{array}{lll} P = P_0 & r \geq r_w & t = 0 \\ q = \dfrac{Q}{2\pi H r_w} & r = r_w & t > 0 \\ q = 0 & r = r_c & t > 0 \end{array} \tag{3}$$

where P_0 [ML^{-1}T^{-2}] is the initial fluid pressure, Q [LT^{-3}] is the volumetric injection rate, H [L] is the formation thickness, r_w [L] is the well radius and r_c [L] is the radial extent of the reservoir unit.

A large time solution for the above problem, when the aquifer is assumed to be infinite in size, is given by Mathias et al. (2008)

$$P_w - P_0 = \frac{Q\mu}{4\pi kH}\left[ln\left(\frac{4kt}{\mu S_p r_w^2}\right) - 0.5772\right] + \frac{Q^2\rho b}{4\pi^2 H^2 r_w} \tag{4}$$

where P_w [$ML^{-1}T^{-2}$] is fluid pressure at the well. Equation (4) is also valid for finite values of r_c.

After pressure perturbation has reached the boundary, the change in pressure with time is relatively uniform (the so-called semi-steady state condition, Dake (1983)), so that

$$\frac{\partial P}{\partial t} = \frac{Q}{AHS_p} \tag{5}$$

where $A = \pi(r_c^2 - r_w^2)$ [L^2] is the plan area of the reservoir unit. Substituting Equation (5) into Equation (2) leads to

$$\frac{Q}{AH} + \frac{1}{r}\frac{d}{dr}(rq) = 0 \tag{6}$$

Substituting in Equation (1), integrating with respect to r and applying the no-flow boundary at $r = r_c$ yields

$$\frac{dP}{dr} = \frac{Q\mu}{2kAH}\left[\left(r - \frac{r_c^2}{r}\right) - \frac{Qk\rho b}{2\mu AH}\left(r - \frac{r_c^2}{r}\right)^2\right] \tag{7}$$

Integration once again and fixing $P = P_w$ at $r = r_w$ leads to

$$\begin{aligned} P - P_w = \frac{Q\mu}{2kAH}\Bigg\{&\frac{r^2 - r_w^2}{2} \\ &- r_c^2 \ln\left(\frac{r}{r_w}\right) + \frac{Qk\rho b}{2\mu AH}\left[2r_c^2(r - r_w) + \frac{r_c^4}{r} - \frac{r_c^4}{r_w} - \frac{r^3 - r_w^3}{3}\right]\Bigg\} \end{aligned} \tag{8}$$

The average reservoir pressure can be obtained from (Dake 1983)

$$\bar{P} = \frac{2\pi}{A}\int_{r_w}^{r_c} rPdr \tag{9}$$

Substituting Equation (8) into (9), evaluating the integral and rearranging for P_w then yields

$$P_w = \bar{P} - \frac{\pi Q\mu}{kA^2H}\left[\frac{r_c^4}{8} - \frac{r_w^4}{8} - \frac{r_c^4}{2}\ln\left(\frac{r_c}{r_w}\right) + \frac{({r_c}^2 - r_w^2)^2}{4} + \frac{Qk\rho b}{2\mu AH}\left(\frac{24r_c^5}{15} - \frac{r_c^6}{2r_w} + \frac{{r_c}^2r_w^3}{2} - \frac{3{r_c}^4r_w}{2} - \frac{r_w^5}{10}\right)\right] \quad (10)$$

Once a semi-steady state is reached, the average pressure can be approximated as $\overline{P} = Qt/AHS_p + P_0$. Recalling that $A = \pi(r_c^2 - r_w^2)$ and assuming $r_c >> r_w$ leads to

$$P_w - P_0 = \frac{Qt}{\pi r_c^2HS_p} + \frac{Q\mu}{2\pi kH}\left[\ln\left(\frac{r_c}{r_w}\right) - \frac{3}{4}\right] + \frac{Q^2\rho b}{4\pi^2H^2r_w}\left(1 - \frac{16r_w}{5r_c}\right) \quad (11)$$

Equation (11) is the solution for a non-Darcy pressure buildup at the well once the semi-steady state conditions become valid.

Further inspection of Equations (4) and (11) suggests that Equation (4) should be further modified to account for non-Darcy effects felt at the far-field boundary such that

$$P_w - P_0 = \frac{Q\mu}{4\pi kH}\left[ln\left(\frac{4kt}{\mu S_pr_w^2}\right) - 0.5772\right] + \frac{Q^2\rho b}{4\pi^2H^2r_w}\left(1 - \frac{16r_w}{5r_c}\right) \quad (12)$$

Under Darcy flow conditions, the late transient transition time, t_0 [T] can be found as a function of the well radius (Dake, 1983). Mathias and Todman (2010) showed that when the flow is governed by the Forchheimer equation, the critical time for the initiation of the late transient approximation is a function of the Forchheimer parameter b and can be found approximately from (Mathias and Todman 2010, Equation (22))

$$t_0 \approx \frac{\mu S_p r_w^2}{k}\left[\frac{1}{(7\cdot 10^3)}\left(\frac{2\pi H r_w \mu}{Qk\rho b}\right)^2 + \frac{1}{(3\cdot 10^7)}\left(\frac{2\pi H r_w \mu}{Qk\rho b}\right)^{1/2}\right]^{-1} \tag{13}$$

The critical time at which the semi-steady state assumption becomes valid, t_c [T] can be found by equating Equation (11) with Equation (12) and assuming that $4kt_c/\mu S_p r_c^2 \ll 1$

$$t_c = \frac{\mu S_p r_c^2}{4k} exp\left(0.5772 - \frac{3}{2}\right) exp\left(\frac{4kt_c}{\mu S_p r_c^2}\right) \approx 0.2423\frac{\mu S_p r_c^2}{k}. \tag{14}$$

It follows that:

- The late transient approximation given in Equation (12) is valid for all times within the interval $t_0 < t < t_c$, where t_0 and t_c are defined in Equations (13) and (14), respectively.
- The semi-steady state solution given in Equation (11) is valid once the influence of the no-flow boundary is felt at the well, i.e. for times $t \geq t_c$.

Note that t_c is not a function of the Forchheimer parameter *b.* Consequently, for smaller reservoir units and dense well networks, there might be no time period when Equation (12) is valid, i.e. the transition straight from the early transient to the semi-steady state flow will occur. Figure 1 shows limiting values of the aquifer size parameters r_c/r_w (for circular domains) and L/r_w (for square domains) at time $t_0 = t_c$, where L [L] represents the length of a square domain. For analysis of domains smaller than critical ones, only the semi-steady state solution given in Equation (11) can be applied. In larger formations, it will take longer before the pressure reaches the boundary, and hence both analytical solutions (11) and (12) can be applied for determination of the pressure at the well.

Multiple wells without the principle of superposition

The nonlinearity in q (see Equation (1)) implies that the principle of superposition is not valid under non-Darcy flow conditions. To solve this problem, an alternative approach to pressure buildup estimation has to be applied.

When analysing equally spaced MWS, well interference has the most significant influence on the pressure buildup at the innermost well in the system (Zakrisson et al. 2008). Moreover, the aquifer hydraulic properties have to be uniform, which implies formation homogeneity. For such a system, the solution for the centrally located (critical) well could provide a limiting value of the pressure buildup, which determines the number and location of wells for a given injection rate. Figure 2 shows a possible layout of an array of equally spaced wells. Due to the interaction between the wells, the central well can be equivalently represented as a single well in a closed square domain of length equal to the well spacing interval.

To account for different geometrical configurations, Dake (1983) presented the general form of inflow equation by introducing the so-called Dietz shape factors (Dietz 1965). This solution is valid only for times when the well is producing under semi-steady state conditions. In this article, it is hypothesised that the centrally located well is adequately represented by a single well situated in a closed circular region of equivalent plan area. Equations (11) and (12) can be applied for the analysis of a square unit of a length L only after the transformation of radius by matching the areas is implemented, such that

$$r_c = \frac{L}{\sqrt{\pi}}. \tag{15}$$

In this way, L represents the well spacing for a grid of equally spaced wells. Mathias et al. (2011) invoke the same assumption for analysing the pressure buildup during CO_2 injection.

Numerical model for two-dimensional non-Darcy flow

To assess the accuracy of the above solution, the response of Equations (11) and (12) was compared to a finite difference solution of the original problem with a genuine square domain. Due to the loss of axial symmetry the problem becomes two-dimensional (2D). Hence, the number of grid-points required becomes squared as compared to numerical simulations previously presented by Mathias et al. (2008).

The continuity equation written for 2D flow takes the form (Wang and Anderson 1995)

$$\frac{\partial q_x}{\partial x} + \frac{\partial q_y}{\partial y} = \delta_{i,j}\frac{Q}{\Delta x \Delta y H} - S_p\frac{\partial P}{\partial t} \tag{16}$$

where x and y [L] are distances along orthogonal axis in the horizontal plane and $\delta_{i,j}$ [-] is a dummy variable that is equal to 1 for a sink or a source term and 0 otherwise. The Forchheimer equation that is used to substitute for q_x and q_y in Equation (16) is linearised by rearranging it such that

$$q_x = -\frac{1}{\frac{\mu}{k} + \rho b|\vec{q}|}\frac{\partial P}{\partial x} \qquad q_y = -\frac{1}{\frac{\mu}{k} + \rho b|\vec{q}|}\frac{\partial P}{\partial y} \tag{17}$$

where $|\vec{q}|$ [LT^{-1}] is a magnitude of a flux vector in radial direction defined as

$$|\vec{q}| = \sqrt{q_x^2 + q_y^2}\,. \tag{18}$$

This leads to the specification of a factor F defined as

$$F = \frac{\mu}{k} + \rho b|\vec{q}| \tag{19}$$

which is treated as a nonlinear coefficient. It is assumed that the factor F is a scalar function of the magnitude of the local flux at any point (Choi et al. 1997). The advantage of this approach to linearisation of the Forchheimer equation is that for insignificant effects of inertial forces, when values of b are close to zero, the factor F converges to μ/k. Consequently, the problem reverts to the simulation of Darcy flow.

Introducing Equation (17) into Equation (16) yields second order linear partial differential equation

$$-\frac{1}{F_i}\frac{\partial^2 P}{\partial x^2} - \frac{1}{F_j}\frac{\partial^2 P}{\partial y^2} = \delta_{i,j}\frac{Q}{\Delta x \Delta y H} - S_p\frac{\partial P}{\partial t}. \tag{20}$$

Starting from an initial guess for pressure head distribution in the considered domain, during each time step the factor F is evaluated using (known) values of pressure from the previous iteration or time step. This allows for Equation (20) to be solved numerically in terms of P at the new iteration level. The results are progressively improving during the iteration process until they approach the exact solution. This procedure is referred to as the Picard iterative method (Stephenson and Radmore 1990).

Whereas Mathias et al. (2008) were able to take advantage of the advanced adaptive time-grid solvers available in MATLAB, the need to solve for many more grid-points means that an alternative and more robust algorithm is required. In this study, Equation (20) is discretised using the finite difference method. To ensure adequate resolution is obtained close to the well, the orthogonal spatial axes are discretised into N logarithmically spaced grid boundary nodes, $x_{B,i}$ and $y_{B,j}$. The grid nodes, x_i and y_j, are placed in the middle of the grid blocks. For simulation of domains of infinite extent, Mathias et al. (2008) found it necessary to discretise the radial dimension into 2000 points. To accurately represent finite domains studied here, 500 points were found to be adequate (therefore the total number of nodes used in each model was 25,000). The time scale is logarithmically discretised as well, to allow for the rapid pressure changes that occur during early times. No-flow boundaries are implemented using image nodes and the injection well is implemented as a sink term at the origin node (*i=1, j=1*). The model is able to represent both circular and square domains within closed boundaries. In the circular model, image nodes are set at the radial distance from the well equal to r_c. The far-field boundary condition for a square unit is set at the constant length of *L/2* in both *x* and *y* directions. A schematic diagram of the numerical grid is presented in Figure 3.

Substituting Equation (17) into Equation (16) and discretising in space and time yields the implicit finite difference approximation for 2D non-Darcy flow

$$a_{i,j}P_{i,j-1}^{n+1} + b_{i,j}P_{i-1,j}^{n+1} + c_{i,j}P_{i,j}^{n+1} + d_{i,j}P_{i+1,j}^{n+1} + e_{i,j}P_{i,j+1}^{n+1} = \delta_{i,j}\frac{Q}{H4x_{i,B}y_{j,B}} + S_p\frac{P_{i,j}^{n}}{\mathrm{t}^{n+1} - \mathrm{t}^{n}} \tag{21}$$

and

$$a_{i,j} = -\frac{1}{\mathrm{F}_{j-1}^{\mathrm{n}}(y_j - y_{j-1})(y_{B,j+1} - y_{B,j})} \tag{22}$$

$$b_{i,j} = -\frac{1}{\mathrm{F}_{i-1}^{\mathrm{n}}(x_i - x_{i-1})(x_{B,i+1} - x_{B,i})} \tag{23}$$

$$d_{i,j} = -\frac{1}{\mathrm{F}_{i+1}^{\mathrm{n}}(x_{i+1} - x_i)(x_{B,i+1} - x_{B,i})} \tag{24}$$

$$e_{i,j} = -\frac{1}{\mathrm{F}_{j+1}^{\mathrm{n}}(y_{j+1} - y_j)(y_{B,j+1} - y_{B,j})} \tag{25}$$

$$c_{i,j} = -a_{i,j} - b_{i,j} - d_{i,j} - e_{i,j} + S_p \frac{1}{\mathrm{t}^{n+1} - \mathrm{t}^n} \tag{26}$$

where $x_{B,i}$ and $y_{B,j}$ [L] are coordinates of grid block boundaries in x and y directions, respectively and x_i and y_j [L] are coordinates of grid nodes in the same directions. This produces the following matrix representation

$$[M^n][P^{n+1}] = [f^n] \tag{27}$$

where *[M]* is a five-diagonal matrix of coefficients defined by Equations (22)-(26) at the previous time step, *[P]* is the pressure vector for $(n+1)^{st}$ time step and *[f]* is a source/sink vector defined as

$$f^n = \begin{cases} S_p \dfrac{P_{i,j}^n}{\mathrm{t}^{n+1} - \mathrm{t}^n} + \dfrac{Q}{H 4 x_{i,B} y_{j,B}} & i = 1, j = 1 \\ S_p \dfrac{P_{i,j}^n}{\mathrm{t}^{n+1} - \mathrm{t}^n} & i = 2 \dots N, j = 2 \dots N \end{cases} \tag{28}$$

Elements of matrix *[M]* are defined to account for influences of the boundary condition. Once determined, coefficient matrices *[a]*-*[e]* are assigned to corresponding diagonals of the matrix *[M]* (Figure 4).

Having defined all elements of implicit numerical scheme approximation, pressures in the next time step are easily obtained as

$$[P^{n+1}] = [M^n]^{-1}.[f^n]\,. \tag{29}$$

Starting with the initial pressure distribution assuming Darcy flow, the first estimation of the nonlinear flow velocity for the next time step is based on values from the previous one. For a given value of b, factor F is obtained using Equation (19). The pressure distribution is then reevaluated in the next iteration, assuming the level of the flow nonlinearity that corresponds to the value of F. If there is significant difference between results in two consecutive iterations, the procedure is repeated with pressure values from the previous iteration as a starting estimate. The iterative procedure is repeated for all defined time steps.

Comparison of solutions

In all simulations, the level of flow nonlinearity was determined by the dimensionless Forchheimer parameter group $Qk\rho b/2\pi H\mu r_w$, having values of 0, 1.59 and 3.18 (representative of typical water production scenarios, see Mathias and Todman, 2010, Table 1). Applied dimensionless transformations allow for results that are independent with respect to parameter values. The numerical scheme is controlled by maximum number of iterations and the error tolerance. In all the simulations presented, error tolerance of 0.001 was used, with a maximum number of iterations set to 1000.

As a first verification, the numerical model is modified to have a circular no-flow boundary by applying image nodes to all nodes at $x^2 + y^2 = r_c^2$. Figure 5 shows plots of dimensionless pressure against dimensionless time at $r = r_w$ for a range of r_c / r_w ratios. Thin black lines and thick grey lines are calculated from Equations (11) and (12) and the finite difference solution, respectively. When $b = 0$, it is clear that there is excellent correspondence between the two solutions, therefore verifying both solutions for Darcy flow in closed circular units. There is also excellent agreement between both solutions for non-Darcy flow, providing times are greater than whichever is the minimum of t_0 and t_c.

Proposed model was finally tested by simulating the original problem of a closed square domain. For same scenarios as shown in Figure 5, analytical solution results were obtained using the effective r_c given in Equation (15). In square domains, the increased rate of pressure buildup, which occurs when the perturbation reaches the boundary (i.e. $t = t_c$), will occur slightly later than in the corresponding circular unit (Figure 6). Again the agreement between the two solutions is excellent, therefore confirming the original hypothesis that square domains are well approximated by circular domains of an equivalent area.

Note that in both Figures 5 and 6, most analytical model results are presented for times $t \geq t_c$. When $t_0 \geq t_c$, the closed boundary affects the well pressure before the late transient solution becomes valid. For such a combination of input parameters, the joint effect of the boundary condition and the non-Darcy flow on the well pressure limits the application of the proposed model to the semi-steady state solution given in Equation (11).

Summary and conclusions

The application of the Forchheimer equation for the modelling of a single-phase flow so far has been limited to infinite aquifers and single-well problems. In this article, the analytical solution for Forchheimer flow to a well in a homogeneous and confined closed aquifer was derived (see Equations (11) and (12)). It was shown that the application of the analytical solutions is constrained by the time when the solution becomes valid. The relation between the aquifer size and transition times was defined, leading to the conclusion that in small aquifers flow conditions will transfer straight from early transient to the semi-steady state.

For linear problems, MWS can be analysed using the principle of superposition. Unfortunately, such an approach is not appropriate for nonlinear problems. In this article, it was hypothesised that MWS can be analysed by finding the pressure buildup at the critical well. That well was treated as a single well in a closed circular formation, with an area equivalent to the zone of influence of the central well in a system of equally spaced wells (see Figure 2 and Equation (15)). Comparison with numerical solution of the full problem verified the accuracy of the approximate solution for all analysed levels of flow nonlinearity.

The application of the proposed solution is limited to confined aquifers. The problem concerning an unconfined aquifer could potentially be modelled using the confined flow equations if a) changes in a water table due to injecting are small relative to the fully saturated thickness of the aquifer (10 % or less (Reilly et al. 1984)) or b) they are embedded with a delayed yield term (Yeh and Chang, 2012). However, the modelling of MWS completed in unconfined aquifers requires further research.

The article develops a framework for the implementation of the Forchheimer equation in transient analytical and numerical models for MWS in confined aquifers. While numerical modelling requires significant computational effort, both in terms of grid and iterative convergence, the analytical solution can be easily applied for the determination of the critical well pressure buildup and MWS analysis. Furthermore, it sets the basis for the analysis of well systems in the presence of hydrological boundaries and points to the possibility of obtaining approximate solutions for alternative non-Darcy problems in closed domains and MWS in the same way (e.g. Mathias et al. 2011).

Notation

A plan area of the reservoir unit, [L^2]

$[a]$-$[e]$	coefficient matrices of the numerical model, (N,N)
b	Forchheimer parameter, [L^{-1}]
c_f	fluid compressibility, [$M^{-1}LT^2$]
c_r	rock compressibility, [$M^{-1}LT^2$]
F	Forchheimer factor, (-)
H	formation thickness, [L]
k	intrinsic permeability, [L^2]
$[M]$	main matrix of the numerical model, (N×N,N×N)
P	fluid pressure, [$ML^{-1}T^{-2}$]
L	length of squared domain/MWS well spacing, [L]
P_o	initial fluid pressure, [$ML^{-1}T^{-2}$]
P_w	fluid pressure at the well, [$ML^{-1}T^{-2}$]
$\bar{P}$	average reservoir pressure, [$ML^{-1}T^{-2}$]
q	fluid flux, [LT^{-1}]
$\lvert\vec{q}\rvert$	magnitude of a flux vector in radial direction, [LT^{-1}]
Q	injection rate, [LT^{-3}]
r	radial distance from the well, [L]
r_c	radial extent of the reservoir unit, [L]
r_w	well radius, [L]
S_p	pressure domain specific storage coefficient, [$M^{-1}LT^2$]
t	time after the beginning of injection, [T]
t_0	late transient transition time, [T]
t_c	semi-steady state transition time, [T]
x_i	coordinates of grid nodes in *x* direction, [L]

y_j coordinates of grid nodes in y direction, [L]

$x_{B,i}$ coordinates of grid block boundaries in *x* direction, [L]

$y_{B,j}$ coordinates of grid block boundaries in y direction, [L]

$\delta_{i,j}$ dummy variable defining sink term, (-)

μ dynamic viscosity, [$ML^{-1}T^{-1}$]

ρ fluid density, [ML^{-3}]

$\emptyset$ formation porosity, (-)

Acknowledgments

The authors would like to acknowledge the support of the Grantham Institute for Climate Change, an Institute of Imperial College London. We also acknowledge the valuable comments by the reviewers of the article, especially Frank A. Spane that greatly improved the manuscript.

References

Bear, J. 1979. *Hydraulics of groundwater*. New York, McGraw-Hill.

Belhaj, H.A., K.R. Agha, A.M. Nouri, S.D. Butt, H.H. Vaziri and M.R. Islam. 2003. Numerical modeling of Forchheimer's equation to describe Darcy and non-Darcy flow in porous media. In: *SPA Asia Pacific Oil and Gas Conference and Exhibition, 15-17 April 2003, Jakarta, Indonesia*. Society of Petroleum Engineers Inc. pp. 1-10, SPE 80440.

Chen, C.S. and C.C. Chang. 2003. Well hydraulics theory and data analysis of the constant head test in an unconfined aquifer with skin effect. *Water Resources Research,* 39(5), 1121-1136.

Chen, C., J. Wan and H. Zhan. 2003. Theoretical and experimental studies of coupled seepage-pipe flow to a horizontal well. *Journal of Hydrology,* 281, 159-171.

Chen, Z, S.L. Lyons and G. Qin. 2001. Derivation of the Forchheimer law via homogenization. *Transport in Porous Media*, 44(2), 325-335.

Choi, E.S., T. Cheema and M.R. Islam. 1997. A new dual-porosity/dual permeability model with non-Darcian flow through fractures. *Journal of Petroleum Science and Engineering*, 17(3), 331-344.

Dake, L.P. 1983. *Fundamentals of Reservoir Engineering*. Elsevier, Netherlands.

Dietz, D.N. 1965. Determination of average reservoir pressure from build-up surveys. *Journal of Petreoleum Technology,* 17(8), 955-959.

Eck, B.J., M.E. Barrett and R.J. Charbeneau. 2012. Forchheimer flow in gently sloping layers: Application to drainage of porous asphalt. *Water Resources Research,* 48(1), W01530.

Ewing, R.E., R.D. Lazarov, S.L. Lyons, D.V. Papavassiliou, J. Pasciak and G. Qin. 1999. Numerical well model for non-Darcy flow through isotropic porous media. *Computational Geosciences*, 3(3), 185-204.

Forchheimer, P. 1901. Wasserbewegung durch Boden. *Z. Ver. Deutsch. Ing.,* 45(1), 1782–1788.

Georgi, T. 1997. Derivation of the Forchheimer law via matched asymptotic expansions. *Transport in Porous Media*, 29(2), 191-206.

Hassanizadeh, S.M. and W.G. Gray. 1987. High velocity flow in porous media. *Transport in Porous Media*, 2(6), 521-531.

Holditch, S.A and R.A. Morse. 1976. The effects of non-Darcy flow on the behavior of hydraulically fractured gas wells. *SPE-5586*, *Journal of Petroleum Technology*, 28(10), 1169–1179.

Irmay, S. 1958. On the theoretical derivation of Darcy and Forchheimer formulas. *Journal of Geophysical Research*, 39(4), 702-707.

Kelkar, M.G. 2000. Estimation of turbulence coefficient based on field observations. *SPE Reservoir Evaluation and Engineering Journal*, 3(2), 160-164.

Kohl, T., K.F. Evans, R.J. Hopkirk, R. Jung and L. Rybach. 1997. Observation and simulation of non-Darcian flow transients in fractured rock. *Water Resources Research,* 33(3), 407-418.

Kolditz, O. 2001. Non-linear flow in fractured rock. *International Journal of Numerical Methods for Heat and Fluid Flow*, 11(6), 547-575.

Lee, J. Y. and K.K. Lee. 1999. Analysis of the quality of parameter estimates from repeated pumping and slug tests in a fractured porous aquifer system in Wonju, Korea. *Ground Water,* 37(5), 692-700.

Legrand, J. 1999. Revisited analysis of pressure drop in flow through crushed rocks. *Journal of Hydraulic Engineering,* 128(11), 1027-1031.

Li, D. and T. Engler. 2001. Literature review on correlations of the non-Darcy coefficient. In *SPE Permian Basin Oil and Gas Recovery Conference, SPE 70015.*

Mathias S.A., G.J. Gonzalez, K.E. Thatcher and R.W. Zimmerman. 2011. Pressure buildup during CO_2 injection into a closed brine aquifer. *Transport in Porous Media,* 89(3): 383-397.

Mathias, S.A. and L.C. Todman. 2010. Step-drawdown tests and the Forchheimer equation. *Water Resources Research,* 46(7), W07514.

Mathias, S.A., P.E. Hardisty, M.R. Trudell and R.W. Zimmerman. 2009a. Screening and selection of sites for CO_2 sequestration based on pressure buildup. *International Journal of Greenhouse Gas Control,* 3(5): 577-585.

Mathias, S.A., P.E. Hardisty, M.R. Trudell and R.W. Zimmerman. 2009b. Approximate Solutions for Pressure Buildup During CO_2 Injection in Brine Aquifers. *Transport in Porous Media,* 79(2): 265-284.

Mathias, S.A., A.P. Butler and H.B. Zhan. 2008. Approximate solutions for Forchheimer flow to a well. *Journal of Hydraulic Engineering,* 134(9): 1318-1325.

Mathias, S.A. and A.P. Butler. 2006. Linearized Richards' equation approach to pumping test analysis in compressible aquifers. *Water Resources Research,* 42(6), W06408.

Mijic, A. and T.C. LaForce. 2012. Spatially varying fractional flow in radial CO_2-brine displacement. *Water Resources Research,* doi: 10.1029/2011WR010961.

Mijic, A. 2009. *Forchheimer flow in multiple well systems*. MSc Dissertation, Imperial College London.

Moutsopoulos, K.N., I.N.E Papaspyros and V.A Tsihrintzis. 2009. Experimental investigation of inertial flow processes in porous media. *Journal of Hydrology*, 374(3), 242-254.

Moutsopoulos, K.N. 2007. One-dimensional unsteady inertial flow in phreatic aquifers induced by a sudden change of the boundary head. *Transport in Porous Media,* 70(1), 97-125.

Nordbotten, J., M. Celia and S. Bachu. 2004. Analytical solutions for leakage rates through abandoned wells. *Water Resources Research*, 40(4), W04204.

Novotny, R. and P. Pech. 2005. Analytical solutions for well drawdown with well losses: 2. Real well near boundary – solution by image well. *Journal of Environmental Hydrology*, 13(28), 1-7.

Pech, P. and R. Novotny. 2005. Analytical solutions for well drawdown with well losses: 1. Multiple well system near a boundary. *Journal of Environmental Hydrology*, 13(27), 1-10.

Qian, J., H. Zhan, W. Zhao and F. Sun. 2007. Experimental evidence of scale-dependent hydraulic conductivity for fully developed turbulent flow in a single fracture. *Journal of Hydrology*, 339(3-4), 206–215.

Qian, J., H. Zhan, W. Zhao and F. Sun. 2005. Experimental study of turbulent unconfined groundwater flow in a single fracture. *Journal of Hydrology*, 311(1), 134–142.

Reddy, N.B.P. and P. Rama Mohan Rao. 2006. Effect of convergence on nonlinear flow in porous media. *Journal of Hydraulic Engineering,* 132(4), 420-427.

Reilly, T.E., O.L. Franke and G.D. Bennett. 1984. *The principle of superposition and its application in ground-water hydraulics.* U.S. Geological Survey.

Ruth, D. and H. Ma. 1992. On the derivation of the Forchheimer equation by means of the averaging theorem. *Transport in Porous Media*, 7(3), 255-264.

Rutqvist J., J.T. Birkholzer and C.F Tsang. 2008. Coupled reservoir–geomechanical analysis of the potential for tensile and shear failure associated with CO_2 injection in multilayered reservoir–caprock systems. *International Journal of Rock Mechanics and Mining Sciences*, 45(2), 132–143.

Schwartz, F.W. and H. Zhang. 2002. *Fundamentals of Ground Water*. Wiley.

Sen, Z. 1988. Analytical solution incorporating nonlinear radial flow in confined aquifers. *Water Resources Research*, 24(4), 601-606.

Sidiropoulou, M.G., K.N. Moutsopoulos and V.A. Tsihrintzis. 2007. Determination of Forchheimer equation coefficients a and b. *Hydrological Processes,* 21(4), 534-554.

Stephenson, G. and P.M Radmore. 1990. *Advanced mathematical methods for engineering and science students*. Cambridge University Press.

Theis, C.V. 1935. The relationship between the lowering of the piezometric surface and the rate and duration of discharge of a well using ground water storage. *Transaction American Geophysical Union,* 16(1), 519–524.

Thiruvengadam, M. and G.N. Pradip Kumar. 1997. Validity of Forchheimer equation in radial flow through coarse granular media. *Journal of Engineering Mechanics*, 123(7), 696–705.

Venkateraman, P. and P. Rama Mohan Rao. 2000. Validation of Forchheimer's law for flow through porous media with converging boundaries. *Journal of Hydraulic Engineering,* 126(1), 63-71.

Venkateraman, P. and P. Rama Mohan Rao. 1998. Darcian, transitional, and turbulent flow through porous media. *Journal of Hydraulic Engineering,* 124(8), 840-846.

Wang, H.F. and M.P. Anderson. 1995. *Introduction to groundwater modelling: Finite difference and finite element methods*. Academic Press.

Whitaker, S. 1996. The Forchheimer equation: A theoretical development. *Transport in Porous Media*, 25(1), 27-61.

Wu, Y.S. 2002a. An approximate analytical solution for non-Darcy flow toward a well in fractured media. *Water Resources Research*, 38(3), 1-7.

Wu, Y.S. 2002b. Numerical simulation of single-phase and multiphase non-Darcy flow in porous and fractured reservoirs. *Transport in Porous Media*, 49(2), 209-240.

Yeh, H.D. and Y.C. Chang. 2012. Recent advances in modeling of well hydraulics. *Advances in Water Resources,* doi: 10.1016/j.adwaters.2012.03.006.

Yildiz, T. 2006. Assessment of total skin factor in perforated wells. *SPE Reservoir Evaluation & Engineering,* 9(1), 61-76.

Zakrisson, J., I. Edman and Y. Cinar. 2008. Multiwell injectivity for CO_2 storage. In *SPE Asia Pacific Oil and Gas Conference and Exibition, SPE 116355.*

Zeng, Z. and R. Grigg. 2006. A criterion for non-Darcy flow in porous media. *Transport in Porous Media*, 63(1), 57-69.

Zimmerman, R.W., A. Al-Yaarubi, C.C. Pain and C.A. Grattoni. 2004. Non-linear regimes of fluid flow in rock fractures. *International Journal of Rock Mechanics and Mining Sciences*, 41(3), 163-169.

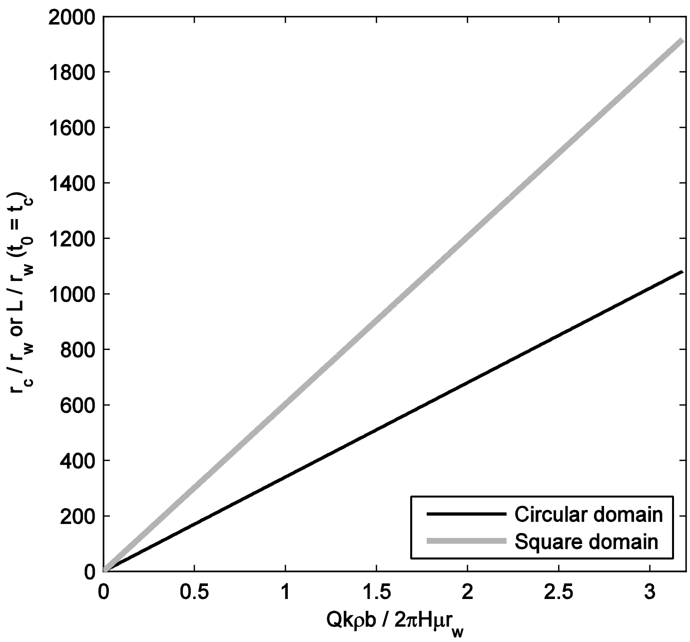

Figure 1: Critical values of aquifer size parameters r_c/r_w (circular domains) and L/r_w (square domains) when t_0=t_c, for a given level of flow nonlinearity

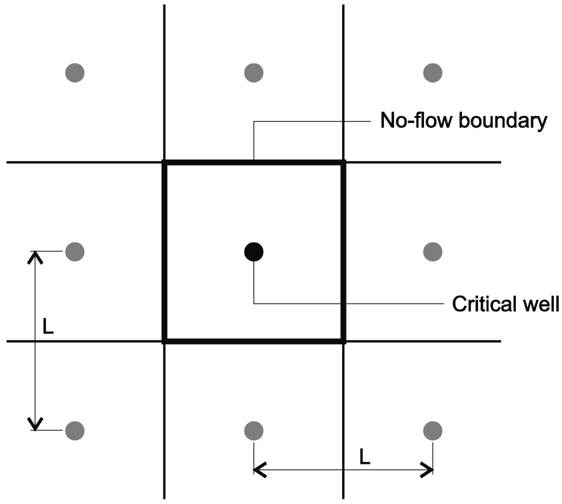

Figure 2: Schematic diagram of a multiple well system

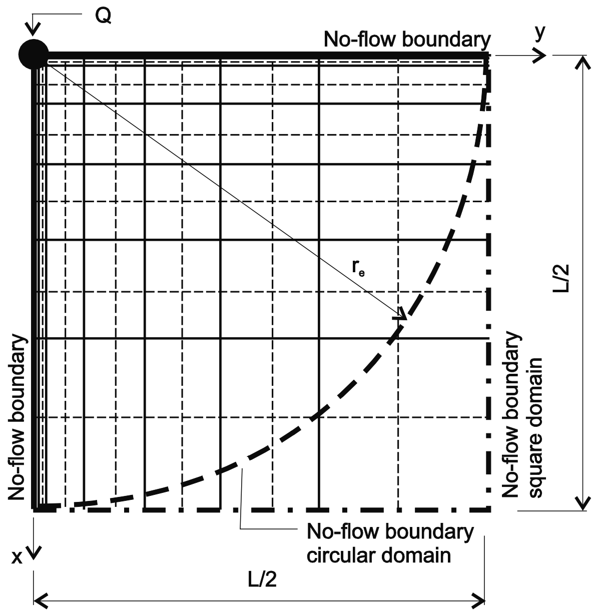

Figure 3: Schematic diagram of the finite difference model

$$
\begin{bmatrix}
c_{1,1} & d_{1,1} & & & e_{1,1} & & & \\
b_{2,1} & c_{2,1} & d_{2,1} & & & e_{2,1} & & \\
 & b_{3,1} & c_{3,1} & d_{3,1} & & & \ddots & \\
 & & b_{4,1} & \ddots & \ddots & & & e_{N,N-1} \\
a_{1,2} & & & \ddots & \ddots & \ddots & & \\
 & a_{2,2} & & & \ddots & \ddots & \ddots & \\
 & & \ddots & & & \ddots & \ddots & d_{N-1,N} \\
 & & & a_{N,N} & & & b_{N,N} & c_{N,N}
\end{bmatrix}
\begin{bmatrix}
P_{1,1} \\ P_{2,1} \\ P_{3,1} \\ \vdots \\ \vdots \\ \vdots \\ \vdots \\ P_{N,N}
\end{bmatrix}
=
\begin{bmatrix}
f_{1,1} \\ 0 \\ 0 \\ \vdots \\ \vdots \\ \vdots \\ \vdots \\ 0
\end{bmatrix}
$$

Figure 4: Implicit numerical scheme in a matrix form

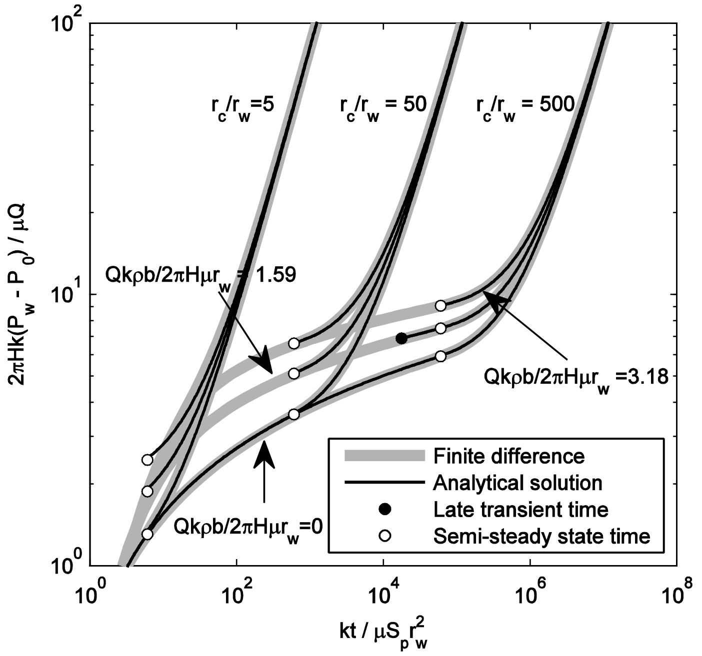

Figure 5: Dimensionless well pressure in a circular domain for various values of r_c/r_w and different levels of flow nonlinearity. Analytical solutions are those given in Equations (11) and (12), only shown within the time range of validity (i.e. for times greater than t_0 or t_c, where appropriate)

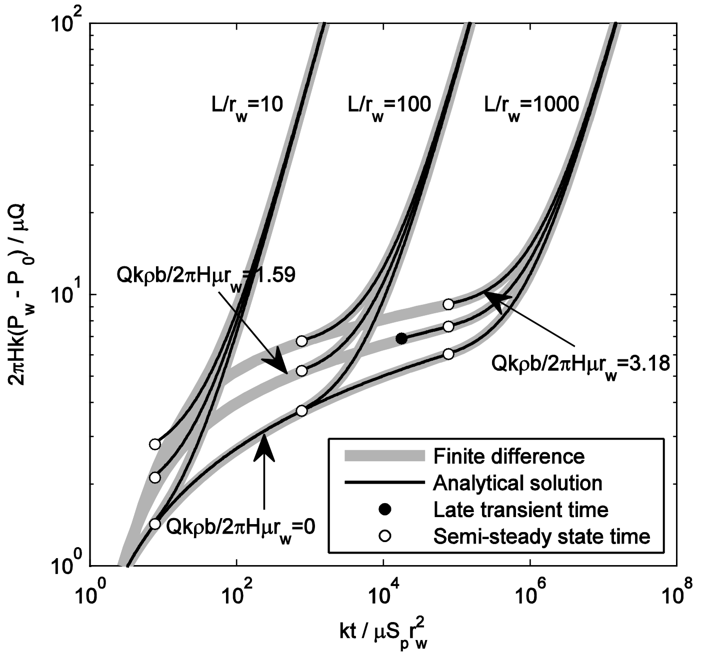

Figure 6: Dimensionless well pressure in a square domain for various values of L/r_w and different levels of flow nonlinearity. Analytical solutions are those given in Equations (11) and (12), with r_c obatined from Equation (15), only shown within the time range of validity (i.e. for times greater than t_0 or t_c, where appropriate)